Research Article

For reprint orders, please contact: reprints@futuremedicine.com

Regenerative Medicine

Adipose-derived human mesenchymal stem cells induce long-term neurogenic and anti-inflammatory effects and improve cognitive but not motor performance in a rat model of Parkinson's disease

Background: Mesenchymal stem cells (MSC) are easily harvested, and possess anti-inflammatory and trophic properties. Furthermore, MSC promote neuroprotection and neurogenesis, which could greatly benefit neurodegenerative disorders, such as Parkinson's disease. **Methods:** MSC were transplanted one week after 6-hydroxydopamine lesioning and effects were evaluated after 6 months. **Results:** MSC localized around the substantia nigra and the arachnoid mater, expressing pericyte and endothelial markers. MSC protected dopamine levels and upregulated peripheral anti-inflammatory cytokines. Furthermore, adipose-derived MSC increased neurogenesis in hippocampal and subventricular regions, and boosted memory functioning. **Conclusion:** Considering that hyposmia and loss of memory function are two major nonmotor symptoms in Parkinson's disease, transplants with modulatory effects on the hippocampus and subventricular zone could provide a disease-modifying therapy.

Keywords: adipose-derived mesenchymal stem cells • adult stem cells • neurogenesis • Parkinson's disease • plasticity • regeneration

Anne Schwerk[1], Jennifer Altschüler[1], Manfred Roch[2], Manfred Gossen[2,3], Christine Winter[4], Jürgen Berg[1], Andreas Kurtz[2,3,5], Levent Akyüz[2,6] & Barbara Steiner*[,1]

[1]Department of Neurology, Charité University Medicine, Berlin, Germany
[2]Berlin-Brandenburg Center for Regenerative Therapies (BCRT), Berlin, Germany
[3]Helmholtz-Zentrum Geesthacht (HZG), Institute of Biomaterial Science, Teltow, Germany
[4]Department of Psychiatry, Technical University Dresden, Germany
[5]Seoul National University, College of Veterinary Medicine & Research Institute for Veterinary Science, Seoul 157–742, Republic of Korea
[6]Institute for Medical Immunology, Berlin, Germany
*Author for correspondence:
Tel.: +49 30 450 517 295
barbara.steiner@charite.de

Parkinson's disease (PD) affects approximately 1% of the population over 60 years of age, making it the most common neurodegenerative movement disorder [1]. The hallmark of the disease consists in the progressive degeneration of dopaminergic neurons in the substantia nigra (SN) and α-synuclein-positive inclusions in cell bodies and neurites (Lewy bodies) of nigral and olfactory bulb (OB) neurons [2,3]. These degenerative processes go together with decreased neurogenesis in the subgranular zone (SGZ) and the subventricular zone (SVZ) – OB axis [4,5]. Furthermore, neurodegeneration in PD has been linked to hyposmia and disease-related cognitive decline [6–8], which are two major nonmotor symptoms related with the majority of PD patients. The decreases in neurogenesis that occur in both neurogenic zones have been attributed to the degeneration of the dopaminergic innervations [4], as demonstrated by several experimental evidences throughout PD models [9]. This suggests that the modulation of endogenous neuronal plasticity in the SVZ-OB axis and in the hippocampus could be a potential regenerative therapeutic target for PD. Many recent studies were built, exploring strategies by either restoring dopaminergic neurons or through the modulation of the proinflammatory microenvironment, which is a part of the pathogenesis in PD [10]. In line with the latter strategy, infused growth factors like GDNF and VEGF [11], and factors counteracting oxidative stress – like erythropoietin (EPO) [12] – showed regenerative and neurogenic effects in PD models. Similarly, other studies transplanted immunomodulatory adult mesenchymal stem cells (MSC) [13] that can naturally secrete trophic factors and cytokines which are important not only for pro- and anti-inflammatory modulation [14,15] but also for the generation and differentiation of newborn neurons in neurogenic regions of the adult brain. In contrast with embryonic or induced-pluripotent stem cells (ipSC), MSC are immunosuppressive and among others have a nontumorigenic potential

Future Medicine part of fsg

upon transplantation [16] and are free of ethical constraints. In addition to their immunosuppressive and trophic properties, MSC are able to home toward the regions of injury [17], which enables them to function as a targeted delivery of trophic factors and cytokines. Given the increase in proinflammatory cytokines and the severe depletion of neurotrophins in PD [18,19], trophic factor secreting MSC could support endogenous repair systems. This was shown in a study conducted in 6-hydroxydopamine (6-OHDA) lesioned rats [20] and Parkinsonian mice [21], whose adult subventricular neurogenesis was increased upon MSC transplantation, along with neuronal precursor cell differentiation in the SN [21]. Similar effects of MSC transplantation were seen on hippocampal neurogenesis [22]. Hence, neurogenic MSC effects might lead to memory improvements and therapeutic effects on olfaction – thereby providing a promising regenerative therapy for nonmotor symptoms in PD.

Adipose tissue contains an abundant vascularization and therefore represents a rich resource of MSC that contains up to 500 times more MSC compared with bone marrow. Furthermore, adipose-derived MSC (AD-MSC) show higher proliferative capacity, later senescence and a higher level of neurotrophin secretion than bone-marrow-derived MSC [23–25]. Our group and others showed recently that AD-MSC improve motor deficits and partially restore dopaminergic marker expression in the striatum and SN [26,27], exert potent immunomodulation [28] and increase brain-derived neurotrophic factor (BDNF) and GFAP levels in the SN [27] of Parkinsonian rats. Furthermore, another short-term study from our lab showed increased neurogenesis upon AD-MSC transplantation in comparison to Parkinsonian rats without AD-MSC treatment [29]. Yet, there is a lack of long-term assessments to ensure the safety of nondifferentiated AD-MSC in the brain and to assess their differentiation and survival. One key issue for long-term studies remains the detection of MSC, given the lack of specific MSC markers that could ensure their tracking and the long-term safety for human applications [30]. Most studies only show human DNA detection [28] or observe a vanishing graft [22,31–35], hindering an assessment of MSC differentiation and development. Consequently, the current study aimed to assess long-term neurogenic, cognitive, immunomodulatory and neuroprotective effects of AD-MSC in respect to their detection, differentiation and homing following transplantation into 6-OHDA lesioned rats.

Materials & methods

Liposuction

After obtaining informed consent from the patient, collected according to the guidelines set by the Ethics Review Board of the Charité University Medicine Berlin, adipose tissue samples were obtained from a 21-year-old female patient during tumescent liposuction. During tumescent liposuction, saline containing anesthetic as well as epinephrine was infused into the subcutaneous tissue through one cannula and then both liquid and tissue were removed with suction.

Isolation & cultivation of AD-MSC

AD-MSC were isolated from adipose tissue by rinsing the tissue samples extensively with 0.1 M phosphate-buffered saline (PBS) containing no magnesium and no calcium ions (Biochrom AG, Berlin, Germany). The fat/ PBS suspension was centrifuged at 350 *g* for 5 min until three layers were obtained. After removing the upper oily layer and the lower aqueous phase, the fatty layer was extracted and digested for 60 min with 0.2 U/ ml collagenase NB4 (Serva Electrophoresis). Subsequently, the sample was centrifuged. The pellet was resuspended in 0.1 M PBS and filtered through a 70 µm strainer. Cells were seeded at a density of 1.6×10^5 cells/cm^2 in DMEM (low glucose; Gibco, UK) culture medium, containing 10% fetal calf serum (Biochrom AG), and 1% penicillin/streptomycin (Invitrogen, Life Technologies, UK).

Detailed methodological descriptions of AD-MSC *ex vivo* expansion, characterization, differentiation and cyto- and immunostaining protocols can be found in the supplementary materials (see online at www.futuremedicine.com/doi/full/10.2217/rme.15.17).

Transfection of AD-MSC

The Neon™ Transfection System (Invitrogen) was used as the nonviral delivery of plasmid DNAs by electroporation. After passage 2, AD-MSC were harvested at 80–90% confluency and diluted in 'resuspension buffer R' (Invitrogen) to a final concentration of 1×10^7 cells/ml. For every transfection, 1 million AD-MSC/100 µl were combined with 4.5 µg of a Sleeping Beauty Transposon encoding the EGFP marker under control of a human elongation factor 1 alpha promoter, as well as SV40 promoter driving expression of a puromycin selection marker, as well as 0.5 µg of the Sleeping Beauty transposase expression vector SB100. Electroporation was set up according to the manufacturer's protocol, applying three pulses of 10 ms each at 1500 V. Afterward, AD-MSC were immediately transferred to standard culture medium. After 48 h, the medium was replaced with puromycin (3 µg/ml) containing medium for 7 days to select for cells with chromosomal integration of the transposon, in other words, green-fluorescent protein (GFP) expressing AD-MSC.

In vivo experimental design

To explore and characterize AD-MSC transplantation into hemiparkinsonian rats and their effects on neurogenesis and regeneration, adult male Wistar rats (n = 40) received 2 µl 6-OHDA or sodium chloride (NaCl) infusions (sham group) into the medial forebrain bundle. Six days after the lesioning, all rats were tested for motor behavior in the rotameter bowels. Seven days later, groups (n = 7/ group) received either 5 µl NaCl or 5 µl of AD-MSC ipsilateral infusions into the SN. Four experimental groups were obtained: sham lesioned animals that received intranigral NaCl injections, 6-OHDA lesioned animals that received intranigral NaCl injections, lesioned animals that received an intranigral injection of AD-MSC (Figure 1). In order to choose the most ideal control group treatment, we based our decision on previous articles in the field [20–21,27,34,36–37] that used NaCl or PBS, however this control group did not reflect the potential to control cell implantation-related impacts.

After AD-MSC or NaCl injections animals received 1 intra peritoneal (i.p.) 5-bromo-2-deoxyuridine (BrdU) injection (50 mg/kg) per day over a 3-day period and were tested again for motor behavior in the rotameter bowels after 4 weeks and a day before their perfusion after 6 months (Figure 1). To assess for memory impairments, the 8-arm maze was used 20 days after lesion induction.

Animals

Adult male Wistar rats were purchased from Harlan Winkelmann Laboratory. Animals were kept under standard housing conditions with a light/dark cycle of 12 h/12 h and with free access to food and water. The study was approved by the local ethic committee 'Landesamt für Gesundheit und Soziales,' Berlin. Suffering of rats was minimized and ameliorated with appropriate anesthetics

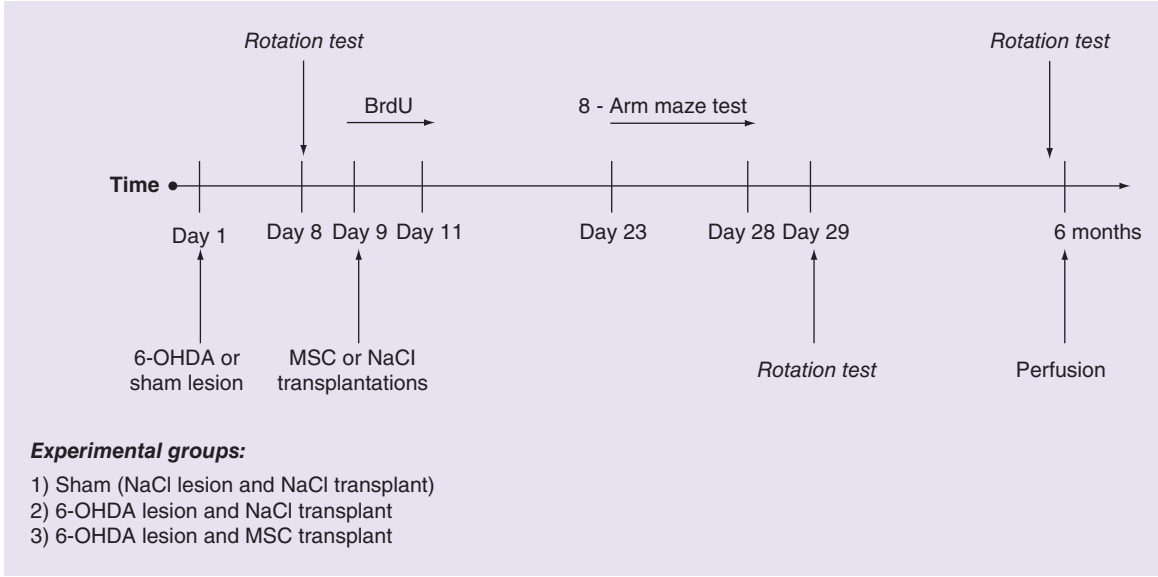

Figure 1. Experimental design. Scheme of experimental setup and groups obtained.
6-OHDA: 6-Hydroxydopamine; BrdU: 5-bromo-2-deoxyuridine; MSC: Mesenchymal stem cell.

6-OHDA lesioning

In order to achieve an end-stage PD model, the medial forebrain bundle was fully lesioned. Stereotaxic operations (David Kopf Instruments, Germany) were carried out under anesthesia with i.p. injections of pentobarbital (60 mg/kg, Sigma Aldrich, Germany). Dopaminergic lesioning was induced by a unilateral 2-point injection of 6.5 µg 6-OHDA (Sigma Aldrich) dissolved in 2 µl saline containing 0.1% ascorbic acid using a 26s gauge Hamilton microsyringe. The following bregma coordinates were chosen: tooth bar (TB): -2.4, anterior–posterior (AP): -4.4, mediolateral (ML): +1.2, dorsoventral (DV): -7.8; and the following interaural coordinates were chosen: TB: +3.4, AP: -4.0, ML: +0.8 and DV: -8.

Intranigral AD-MSC transplantation

Stereotaxic operations (David Kopf Instruments) were carried out under deep anesthesia with i.p. injected pentobarbital (60 mg/kg, Sigma Aldrich). Three hundred thousand cells were infused with a 20-gauge Hamilton microsyringe over a rate of 2 min and retracted after 5 min. Intranigral infusion was based on the following bregma coordinates: TB: -3.3, AP: -5.3, ML: 2.4 and DV: -7.4 (supplementary Figure S5).

Quantification of endogenous neurogenesis in the SVZ & dentate gyrus

Total diaminobenzidine (DAB; Sigma Aldrich) BrdU in the SVZ (including the lateral wall of the ventricles) was quantified by counting one-in-six series, resulting in six coronal sections from the appearance of the third ventricle (1.70, anterior to bregma) to the disappearance of the anterior commissure (-0.4, posterior to bregma). Similarly, one-in-six series of DAB BrdU stained cells were counted in the SGZ and granule cell layer of the dentate gyrus (DG), resulting in eight sections per animal. Obtained numbers were then multiplied by 6 in order to estimate the total number of BrdU-immunoreactive cells.

Fluorescent staining of the SVZ was visualized and quantified with a confocal microscope (Leica TCS SP2) at 40× magnification. For each group (n = 5), 40-µm thick sections were stained and the total number of BrdU-positive cells (BrdU+) was counted. Double positive cells, for BrdU and HuD cells (BrdU+/ HuD+) were quantified to assess neurogenesis, and double positive cells for BrdU and S100β (BrdU+/ S100β+) were quantified to assess gliogenesis on each hemisphere in two subregions of the SVZ, the lateral ventricle and the beginning of the rostral migratory stream. BrdU+/ HuD+ and BrdU+/ S100β+ and total BrdU cell numbers were counted in every 6th section and selected regions were analyzed in sequential scanning mode. Ratios of double-labeled cells versus all BrdU+ cells are given.

Quantification of dopaminergic neurons

To verify the lesion, TH+ neurons were counted in the SN. Stereological cell counts of TH+ neurons in the SN were based on anatomical landmarks, as described in Tepper *et al.* [38] and according to Paxino and Watson [39]. To circumvent arbitrary delineation, the whole of the rostrocaudal extent of the SN (including the pars compacta, pars reticulata and pars lateralis) were counted using the 'Meander Scan' option and a semi-automated stereology system (StereoInvestigator, MicroBrightfield, VT, USA) employing a Leica DMRA microscope attached to a Retiga-2000R camera (QImaging, Canada). One-in-twelve series of 40 µm coronal sections were evaluated for each group (n = 7) resulting in four sections in total. The SN was delineated using the 5× objective, while counting was done at the 40× objective. All cell counts were executed by the same investigator in a blind manner. The coefficient of error (ranging between 0.05 and 0.1) without the estimation bias of the total numbers was calculated according to Gundersen and Jensen. For quantification, TH+ cell numbers were expressed as percentage of the nonlesioned side. The grid was determined manually based on the shape of the SN. The counting frame is determined automatically based on the grid size. For the counting of TH+ cells in the SN, four coronal sections of 40 µm were used per animal.

Quantification of inflammatory response

In order to determine the (peripheral) inflammatory response to the transplantation, all rat sera and conditioned media were analyzed for the presence of various cytokines, chemokines and growth factors, using multiplex assay kits and Luminex technology (BioSource/ Invitrogen, Germany). Rat sera were collected at the time of the perfusion. A rat 22-plex kit was designed to test for angiogenic (VEGF, monocyte chemoattractant protein-1) and hematopoietic cytokines/ chemokines (granulocyte colony-stimulating factor, granulocyte macrophage colony-stimulating factor, macrophage colony-stimulating factor, IL-5, IL-7) and for pro- (TNF-α, human growth-regulated oncogene/ keratinocyte chemoattractant, IFN-γ, IL-1α, IL1β, IL-12p70, IL-17α, IL-6, IL-18, regulated upon activation normal T-cell expressed and secreted, macrophage inflammatory protein-3α) and anti-inflammatory cytokines/chemokines (EPO, IL-10, IL-4, IL-13). All procedures were carried out according to the manufacturer's instruction. Briefly, 50 µl of undiluted serum was added to wells containing antibody coated beads and incubated for 2 h at room temperature. The beads

were washed and incubated with biotinylated detector antibody for 1 h, then washed again and incubated with streptadivin-RPE for 30 min. After another wash, fluorescence was detected using a Luminex-100 instrument and analyzed with proprietary software. The amount of each cytokine in picoG/ml was used for comparisons between groups. A highly specific cytokine kit was chosen that was tested negative for human cross-reactions.

Behavioral tests

Seven days before the start of the experiments, animals were handled for approximately 2 min daily. All experiments were carried out between 8:00 and 12:00 am. Before each trial, the radial maze and conditioning chamber were cleaned with water, and rotameter bowls were cleaned with water containing 30% ethanol. In order to reduce stress and novelty seeking behavior, animals were transported in their home cage and allowed to habituate for 30 min prior to the start of the experiments.

D-amphetamine-induced rotations

Rotational response to D-amphetamine is a classic functional measure of unilateral dopaminergic denervation [40]. One week post-lesion (day 8), 20 days post-grafting (day 29) and after 6 months, animal rotational behavior was tested in response to D-amphetamine sulfate injection (2725 mg/kg dissolved in 0.9% saline i.p., Sigma Aldrich). Animals were injected and placed into automated rotameter bowls (TSE Systems, Germany). The number of turns performed by the animals greater than 180° was recorded for 90 min starting 15 min after injection.

Eight-arm radial maze

The test was conducted according to a previous protocol [41] with slight modifications. The radial arm maze was constructed of dark gray polyvinylchloride and consisted of an octagonal center platform (50 cm in diameter) and eight equally spaced arms radiating from the octagon (42 cm long and 10 cm wide). A semicircular food cup, 3 cm in diameter and 1 cm deep, was located at the outer end of each arm in order to present a food reinforcer that is to say a quarter of a peanut. The apparatus was placed centrally on the floor of the experimental chamber which was uniformly and indirectly lit with 4 40W bulbs and had white walls. Furthermore, the experimental room was equipped with visible extra-maze cues that remained constant during the study to allow spatial orientation. Three days before the experiment, food deprivation was initiated and kept throughout the test. The rats were fed 2 h per day – with water ad libitum – in order to reduce their body weight to approximately 85% of the initial value. Body weight was monitored on a daily basis. During the first 2 days of the 8-day testing period, rats were habituated to the maze and trained to find the reinforcers. All arms were baited and animals were individually placed in the center of the maze for the duration of 10 min. In the course of the subsequent 6 days memory tasks were performed. During this test phase, only the arms, which were directed toward the extra cues, were baited with constant location between trials. The rats were free to explore the maze and remained on the maze either until all three rewards had been eaten or until 10 min had elapsed. The first entry into an unbaited arm was scored as reference memory error (RME), any arm re-entries (either in a formerly baited or unbaited arm) were scored as working memory error (WME). The test was conducted from day 21 to day 28 after the 6-OHDA lesion.

Statistical analyses

Data were presented as mean and standard error of the mean with the significance level set at $p = 0.05$. Group comparisons were analyzed with an analysis of variance (ANOVA), repeated measurements ANOVA (rmANOVA) and multivariate ANOVA (MANOVA), followed up with least significant difference (LSD) or Tamhanes posthoc comparisons using SPSS (IBM, version 22). In some tests (Multiplex and SVZ DAB BrdU analyses), data were transformed to the logarithm of the basis 10 (log10) to normalize the skewed distribution.

Results

AD-MSC secrete VEGF *in vitro* & increase peripheral EPO & Il-10 levels *in vivo*

Multiplexed analyses of 22 pro- and anti-inflammatory cytokines and chemokines were applied to all rat sera and to culture medium of AD-MSC. Only VEGF, a potent factor for the induction of vasculogenesis and angiogenesis, was found to be elevated in AD-MSC medium compared with unconditioned medium.

Serum analyses indicated that EPO levels were significantly different between groups [$F(2, 22) = 6.55$, $p = 0.01$, partial $\eta^2 = 0.37$]; posthoc comparisons showed significantly higher EPO levels in AD-MSC versus 6-OHDA ($p = 0.002$) and higher EPO levels in sham versus 6-OHDA ($p = 0.02$). Furthermore, log10 transformed IL-10 levels were significantly different between groups [$F(2, 24) = 6.45$, $p = 0.006$, partial $\eta^2 = 0.35$], LSD posthoc tests showed significant higher IL-10 levels in AD-MSC ($p = 0.01$) and sham ($p = 0.01$) as compared with 6-OHDA. Log10 transformed IL-2 levels were also found to be different between groups [$F(2, 18) = 5.00$, $p = 0.02$,

partial $\eta^2 = 0.36$], showing higher levels in AD-MSC as compared with 6-OHDA ($p = 0.01$) at posthoc. Log10 transformed IL-4 was also significantly different between groups [$F(2, 23) = 7.49$, $p = 0.003$, partial $\eta^2 = 0.39$], showing higher levels in AD-MSC ($p = 0.001$) and sham ($p = 0.02$) as compared with 6-OHDA (Figure 2 & Supplementary Table S3). In all analyses, there were no significant differences between sham and AD-MSC treated animals.

Nigral transplantation of AD-MSC induces long-term survival of newborn subventricular neurons

BrdU immunoreactivity of SVZ cells showed significant different amounts of ipsilateral BrdU+ cells between groups [$F(2, 25) = 3.73$, $p = 0.04$, partial $\eta^2 = 0.23$]. LSD posthoc comparisons showed significantly more BrdU+cells ($p = 0.01$) in sham control rats [n = 7, BrdU: 2472 (1327)] as compared with6-OHDA lesioned animals [n = 7, BrdU: 1204 (403)]. There was no difference in absolute BrdU numbers of AD-MSC transplanted animals [n = 14, BrdU: 1717 (916)] as compared with sham or 6-OHDA (Figures 3A & 4A–D).

Quantification of BrdU+/ HuD+ cells showed significant differences in the numbers of neurons generated in the first 3 days and surviving up to 6 months after transplantation [$F(2, 25) = 7.17$, $p = 0.003$, $\eta^2 = 0.36$]; AD-MSC groups showed significantly more BrdU+/ HuD+ neurons compared with 6-OHDA groups ($p = 0.003$), and sham animals showed significantly more BrdU+/ HuD+ cells than 6-OHDA ($p = 0.04$) (Figures 3B & 5A–C, and Table 1). Indicating that both AD-MSC and sham transplanted animals had higher numbers of newly generated surviving neurons compared with 6-OHDA, while there was no difference between sham and AD-MSC.

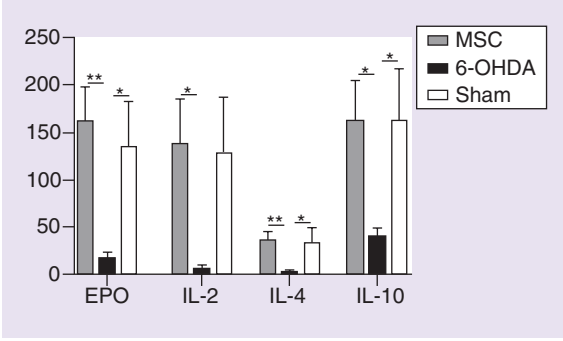

Figure 2. Multiplex ELISA. Bar chart showing mean levels of EPO, IL-10, IL-4 and IL-2. Significant higher EPO ($p = 0.002$), IL-10 ($p = 0.01$), IL-4 ($p = 0.001$) and IL-2 ($p = 0.01$) were observed in a dipose-derived-MSC compared with 6-OHDA treatment. Sham animals showed significantly higher EPO ($p = 0.02$), IL-4 ($p = 0.02$) and IL-10 levels ($p = 0.01$) compared with 6-OHDA animals. Data are presented in pg/ml as mean and standard error of the mean.
** indicating $p < 0.005$; * indicating $p < 0.05$.
6-OHDA: 6-Hydroxydopamine; MSC: Mesenchymal stem cells.

Transplantation of AD-MSC induces long-term increases in hippocampal neurons

After 6 months of transplantation, surviving BrdU+ cells in the SGZ of the hippocampus showed significant different amounts of total BrdU-immunoreactive cells between groups [$F(2, 16) = 14.7$, $p = 0.000$, partial $\eta^2 = 0.65$]. LSD posthoc comparisons showed significantly more BrdU+cells in AD-MSC treated rats as compared with 6-OHDA ($p = 0.04$), and in sham control rats as compared with6-OHDA lesioned animals ($p = 0.04$) (Figures 3A & 6A–D, and Table 1).

AD-MSC localize in the arachnoid mater & around blood vessels

After 6 months of transplantation, all AD-MSC lost their GFP-expression, but could be phenotypically identified by robust human-specific marker expression of HuMi, MHC-I, and CD44 (Figures 7A–E & 8). In our previous short-term studies, AD-MSC showed a marked reduction in GFP expression already after 4 days of transplantation, suggesting a progressive loss of GFP expression in AD-MSC transplants (data not shown).

Most AD-MSC were found in the arachnoid mater, often close to the SN. AD-MSC expressed CD34 (Figures 8A–J), von Willebrandt Faktor (Figure 8F–J), SOX2 (Figure 8K–O) and BDNF (Figure 8P–T) but showed no vimentin expression, which is indicative of the MSC lineage. In addition, AD-MSC expressed NG2 (Figure 8U–Y), a marker for polydendrocytes and pericytes. Neuronal markers, like doublecortin and β-tubulin-III were not expressed by AD-MSC (Figure 8S & X, respectively).

AD-MSC transplantation reduces dopaminergic degeneration in the SN

There was a significant difference in TH+ neurons between groups [$F(2, 25) = 26.61$, $p < 0.000$, partial $\eta^2 = 0.68$]. LSD posthoc comparisons showed significantly higher TH levels in AD-MSC compared with 6-OHDA ($p = 0.000$), and higher TH levels in sham animals compared with AD-MSC ($p = 0.000$) and 6-OHDA ($p = 0.000$) (Figure 9A–D, Table 1). Furthermore, the amount of subventricular BrdU+/HuD+ neurons correlated positively (n = 28, $\rho = 0.40$, $p = 0.03$) with the amount of TH+ neurons in all groups, indicating a relationship between dopaminergic neurons and subventricular neurogenesis. There were no BrdU+/ TH+ neurons in the sham, 6-OHDA, or AD-

MSC group, implicating an absence of dopaminergic neurogenesis, after 6 months of transplantation. Also no human TH+ cells were seen, showing the lack of dopaminergic transdifferentiation of AD-MSC.

AD-MSC transplantation improves working memory in the radial-arm-maze test

When analyzing WME of the six trials, there was a significant main effect of WME [F (5, 21) = 8.79, p = 0.000, partial η^2 = 0.68], indicating learning of all groups. There was also a significant interaction of group membership and WME [F (10, 44) = 2.13, p = 0.04, partial η^2 = 0.33], which indicated that at the first test day, sham scored better than 6-OHDA (p = 0.005), and also at day 2 sham performed better than 6-OHDA (p = 0.006) and AD-MSC (p = 0.05), yet there was no difference at day 3. However, from day 4 onward AD-MSC showed fewer WME than 6-OHDA (day 4: p = 0.001; day 5: p = 0.000; day 6: p = 0.000) and sham animals showed also continuously a better performance than 6-OHDA (day 4: p = 0.000; day 5: p = 0.000; day 6: p = 0.000) (Figure 10A, Table 2).

When analyzing RME, there was only a significant main effect of RME [F (5, 21) = 8.73, p = 0.000, partial η^2 = 0.68] indicating a learning effect for all groups. Taken together, these data show that all groups were able to improve their short-term and reference memory over time, yet the 6-OHDA group showed impairments in short-term memory (WME) as compared with both sham and AD-MSC groups – indicating that AD-MSC transplantation improved working memory performance in lesioned animals.

AD-MSC treatment does not improve motor function in PD animals

When comparing the rpm over the three test dates, rmANOVA showed no significant interaction between group and rotation test days (p = 0.85), and no difference across test days (p = 0.08), but a significant difference of treatment condition [F (2,23) = 4.89, p = 0.02, partial η^2 = 0.30), indicating that sham animals turned significantly less over the three test days compared with AD-MSC (p = 0.02) and 6-OHDA (p = 0.007) (Figure 10B).

Discussion

In the present study, viable AD-MSC descendants were detectable up to 6 months following intranigral transplantation in the 6-OHDA lesioned rat brain and exerted beneficial effects on adult neurogenesis in the SVZ and DG, memory function, TH-levels, and on peripheral cytokines. AD-MSC localized often around blood vessels or in the arachnoid mater – two

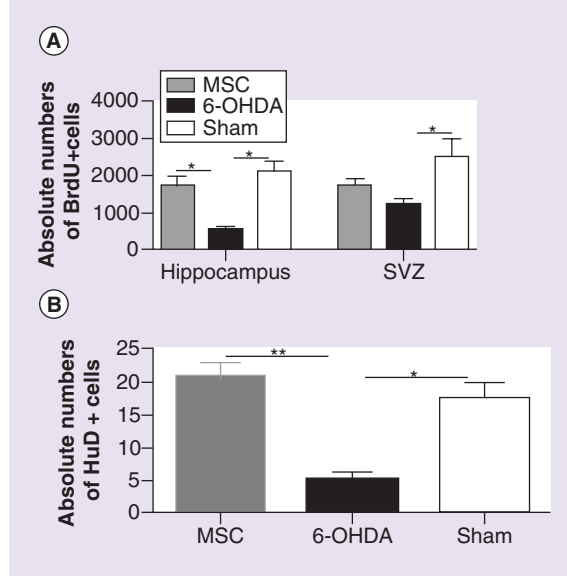

Figure 3. Quantitative histological analysis of newly generated subventricular and hippocampal cells. **(A)** Analysis of variance showing significantly increased subventricular BrdU+ cells in sham transplanted animals (n = 7) versus 6-OHDA (n = 7, p = 0.01) and no differences between adipose-derived (AD)-MSC and sham or 6-OHDA treatment. The numbers of BrdU+ cells in the dentate gyrus were significantly higher in AD-MSC transplanted animals compared with 6-OHDA (p = 0.04), and compared with sham transplanted animals versus 6-OHDA (p = 0.04). **(B)** Analysis of variance showing significantly increased BrdU+/HuD+ neurons in AD-MSC (n = 14) transplanted animals versus 6-OHDA (n = 7, p = 0.003) and in sham transplanted animals (n = 7) as compared with 6-OHDA (p = 0.04).
** indicating p < 0.005; * indicating p < 0.05.
6-OHDA: 6-Hydroxydopamine; BrdU: 5-Bromo-2-deoxyuridine; MSC: Mesenchymal stem cells; SVZ: Subventricular zone.

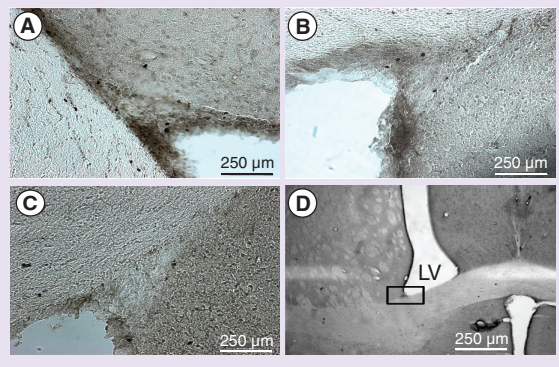

Figure 4. Histochemical stainings of neurogenesis in the subventricular zone. The pictures are showing 5-bromo-2-deoxyuridine+ cells in **(A)** the subventricular zone of sham, **(B)** adipose-derived mesenchymal stem cell and **(C)** 6-hydroxydopamine animals. **(D)** Overview of the subventricular zone, rectangles are indicating sampling fields. The 2.5x objective was used for **(D)**, the 20x objective was used for **(A-C)**.

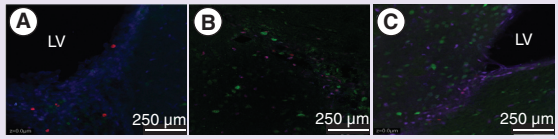

Figure 5. Neurogenesis in the subventricular zone.
The pictures are showing neuro- and gliogenesis in the subventricular zone of **(A)** 6-Hydroxydopamine, **(B)** adipose-derived mesenchymal stem cell, and **(C)** sham infused animals. Neurons were stained with anti-HuD (green), astrocytes with S100β (blue) and newly generated cells with 5-bromo-2-deoxyuridine (red). The 20x objective was used for all.
For color images please see online www.futuremedicine.com/doi/full/10.2217/RME.15.17

microenvironments that provide a protective microenvironment for the survival and differentiation of resident and exogenous stem cells due to their stem cell niche-like characteristics [42–44], and due to circulating growth factors [45,46].

We assume that AD-MSC indeed increased the generation and survival of neurons in the dentate gyrus, considering that it was shown previously that 4 weeks after injecting BrdU into mice, the vast majority of BrdU+ cells express neuronal phenotype markers [47]. The increased hippocampal neurogenesis of AD-MSC treated versus nontreated Parkinsonian animals was functionally related with improved memory test performance, as shown by significantly less WME made by AD-MSC versus 6-OHDA animals. This is in line with prior studies showing working memory deficits upon 6-OHDA lesioning [48]. Cognitive decline is a main nonmotor symptom of PD [49] that predisposes the majority of patients to progress to dementia [50], underlining the relevance of early neuroprotective and potentially disease-modifying treatment strategies. Furthermore, not only hippocampal neurogenesis was increased but also also subventricular neurogenesis, characterized by BrdU+/ HuD+ neurons, was about 15% higher in AD-MSC treated animals compared with 6-OHDA lesioned untreated animals, while there was no difference between sham and AD-MSC, indicating a normalizing effect of AD-MSC treatment on subventricular neurogenesis. Similar results were found in our previously published short-term study, which showed higher neurogenesis in the SVZ of AD-MSC treated rats versus only 6-OHDA lesioned rats [29]. Both of these neurogenic zones show decreased numbers of neurons going along with α-synuclein positive inclusions in PD patients [4,5], which have been linked to dopaminergic denervation [4]. Furthermore, neuronal loss in the OB showed a strong correlation with disease duration in PD [5], implicating a progressive degeneration of OB neurons. Hence therapeutic modulation of endogenous plasticity in the SVZ-OB axis with vehicles like AD-MSC might present a promising treatment strategy in PD that could help restore the OB and hippocampal neurogenesis, going along with hyposmia and cognitive decline. In line with previous studies [4], we found a positive correlation between the amount of subventricular BrdU+/ HuD+ neurons and the amount of dopaminergic neurons in all groups, indicating a relationship of increased neurogenesis with increased dopaminergic tone. We assume not only an interaction of the transplanted AD-MSC with the local microenvironment inducing neuroprotection on one hand but also the generation of newborn neurons on the other hand, as shown in previous recent studies from our group. Furthermore, our colleagues showed a profound effect of AD-MSC on TH and BDNF levels and on motor behavior in Parkinsonian rats [27].

Table 1. Summary of histological findings.

Type	AD-MSC	Sham control	6-OHDA lesion	Statistics
Surviving neurons in the subventricular zone after 6 months of transplantation				
BrdU+	1717(916) n = 14	2472(1327) n = 7, p =0.01†	1204(403) n = 7	F(2, 25) = 3.73, p = 0.04, partial η^2 = 0.23
BrdU+/HuD+	15(7)% n = 14, p =0.003‡	13(6)% n = 7, p =0.04†	4(2)% n = 7	F(2, 25) = 7.17, p = 0.003, partial η^2 = 0.36
Hippocampal neurogenesis after 6 months				
BrdU+	1749(611) n = 7, p = 0.04‡	1749(611) n = 7, p = 0.04‡	530(172) n = 6	F (2, 16) = 14.7, p = 0.000, partial η2 = 0.65
Dopaminergic neuron survival				
Ipsilateral TH+ cells	64(18) n = 14, p = 0.000‡	94(6) n = 7, p = 0.000†,§	37(10) n = 7	F (2, 25) = 26.61, p = 0.000, partial η2 = 0.68

†Indicating significant differences between sham control vs 6-OHDA.
‡Indicating significant differences between AD-MSC vs 6-OHDA.
§Indicating significant differences between AD-MSC vs sham control.
6-OHDA: 6-Hydroxydopamine; AD-MSC: Adipose-derived mesenchymal stem cells; BrdU: 5-Bromo-2-deoxyuridine.

The protection of dopaminergic neurons in 6-OHDA lesioned animals following AD-MSC treatment might be supported by local microenvironmental changes, stimulated by altered cytokines levels and growth factors, as IL-10, whose transgenic expression was shown to protect TH levels in the SN and in the striatum of 6-OHDA lesioned rats [51]. Yet, there was still no complete histological recovery in our study, which might have caused the lack of motoric amelioration that was measured with rotational performances. Furthermore, our results suggest that AD-MSC transplantation affects cognition and anti-inflammatory parameters that eventually lead to neuroprotection, rather than motor behaviour. However, the outcomes of the rotational performances must be interpreted with caution, as they reflect only few Parkinsonian symptoms in the 6-OHDA model and as they show low external validity [52,53]. In addition, there is no linear correlation of rotational performances and dopamine loss or recovery of dopamine [54]. This raises the possibility that rotometry might not cover the amelioration achieved by AD-MSC and suggests that upcoming studies should employ a battery of motor behavior test or employ more sensitive motoric tests [53]. Another limitation encountered in our study design was the lack of an appropriate control group that reflects any potential cell implantation-related impact, for example, nontrophic factor secreting fibroblasts. Therefore, future studies should address this requirement with more rigors.

In the present study, several cytokines/chemokines were found to be decreased by 6-OHDA, while there were similar in AD-MSC and sham lesioned animals, indicating a normalizing effect of AD-MSC treatment. Yet, higher IL-10, IL-4 and IL-2 are also elevated in allograft reactions, considering that we found viable and functionally intact MSC, with similar cytokine levels as sham, we do not assume that the elevation is due to an allograft reaction. Rather we found that AD-MSC significantly increased factors related to the modulation of neurogenesis, leading to similar cytokine levels as measured in sham treated controls. EPO – a growth factor for hematopoietic progenitor cells – has been shown to lead to antiapoptotic, antioxidant and anti-inflammatory effects on neurons, glial and endothelial cells and to stimulate angiogenesis and neurogenesis and the migration of neuroblasts [55,56]. Also, the anti-inflammatory IL-10, known to modulate adult neurogenesis [57,58], was elevated upon AD-MSC transplantation. The stimulation of these exemplary factors supports the hypothesis of AD-MSC-induced neurogenesis through changes in the local microenvironment of the lesioned brain and show in general, as a proof of principle, that the microenvironment in the Parkinsonian brain is modulated by AD-MSC, with resulting neurogenic and neuroprotective effects.

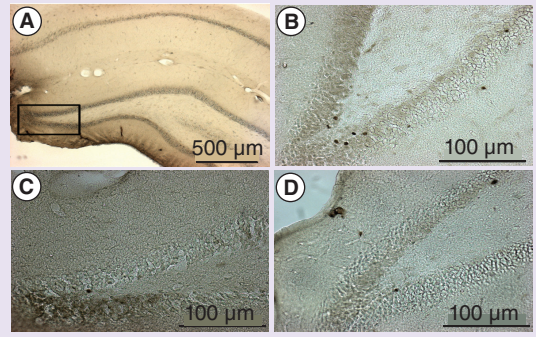

Figure 6. Neurogenesis in the dentate gyrus.
(A) An overview of the dentate gyrus, rectangles are indicating sampling fields. Newly generated cells in the subgranular zone and molecular layer of the dentate gyrus in the hippocampus of **(B)** adipose-derived mesenchymal stem cells, **(C)** 6-Hydroxydopamine and **(D)** sham transplanted animals. The 2.5× objective was used for **(A)**, the 20× objective was used for **(B–D).**

The demonstrated neurogenic and neuroprotective effects of AD-MSC in our study might also be supported by their *in vivo* BDNF expression, which has a well-known role in supporting neurogenesis and providing trophic supply to dopaminergic neurons. After transplantation, AD-MSC were rather characterized by the expression of neurotrophic (BDNF), pericytical (NG2, CD34) and endothelial markers (von Willebrandt Faktor), eventually indicating a fusion with other endogenous cells, as it has been shown

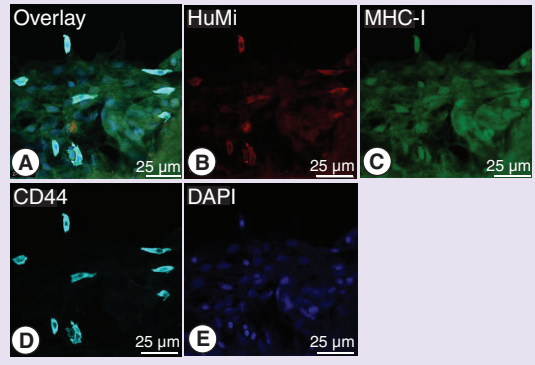

Figure 7. Tracking of adipose-derived mesenchymal stem cells *in vivo* after 6 months. (A) Overlay ofadipose-derived mesenchymal stem cells after 6months showing **(B)** HuMi (red), **(C)** MHC-I (green), **(D)** CD44, and **(E)** DAPI+ cell nuclei (blue). The 40x objective was used for all.
DAPI: 4, 6-Diamidino-2-phenylindole; HuMi: Antihuman mitochondria.
For color images please see online www.futuremedicine.com/doi/full/10.2217/RME.15.17

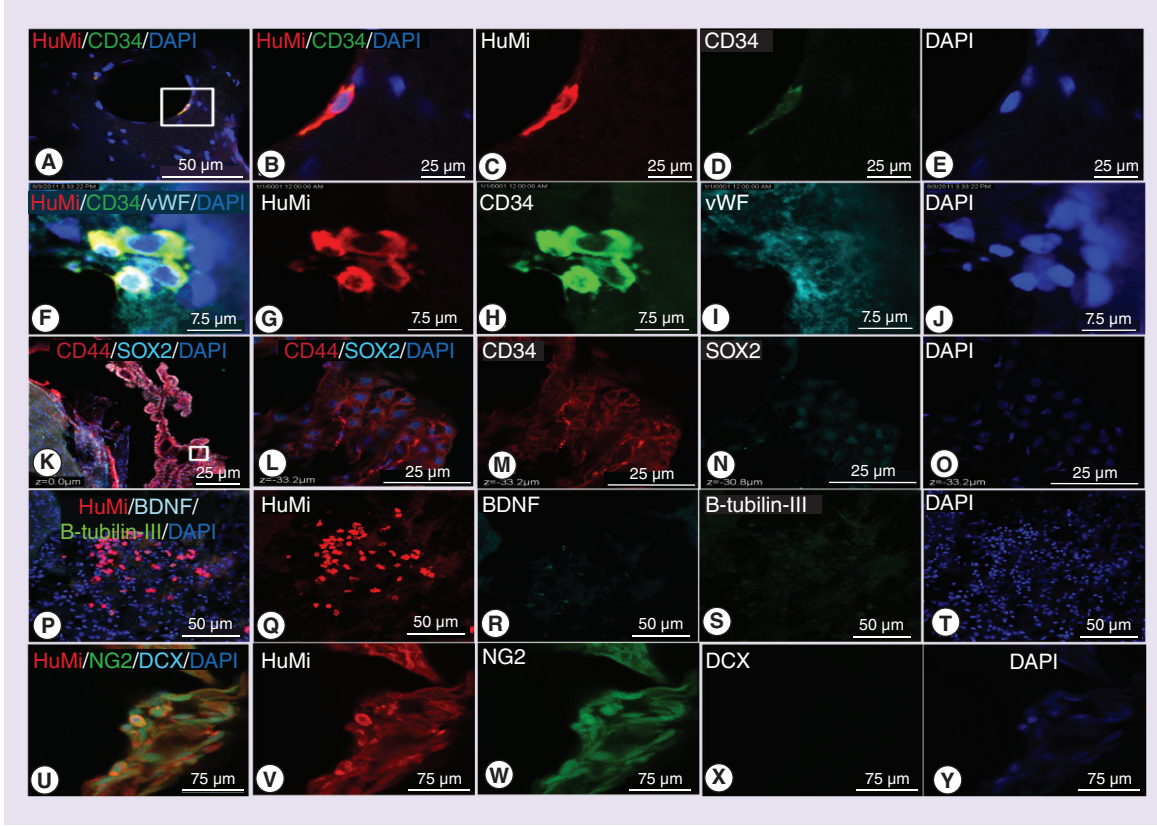

Figure 8. Characterization of adipose-derived mesenchymal stem cells *in vivo* after 6 months of transplantation. **(A&B)** Overlay with **(B)** indicating a magnification of **(A)**, showing **(C)** HuMi, **(D)** CD34 and **(E)** DAPI expression of AD-MSC. **(F)** AD-MSC overlay showing their labeling with **(G)** HuMi, **(H)** CD34, **(I)** vWF, and **(J)** DAPI. **(K&L)** Two overlays with **(L)** indicating a magnification of **(K)**, showing AD-MSC in the arachnoid mater, expressing **(M)** CD44, **(N)** SOX2, and **(O)** DAPI. **(P)** Overlay showing **(Q)** HuMi-labeled AD-MSC, **(R)** positive for BDNF and DAPI, but **(S)** negative for the neuronal marker β-tubulin-III. **(U)** Overlay depicting **(V)** HuMi-positive AD-MSC in the arachnoid mater, expressing **(W)** NG2 and **(Y)** DAPI but **(X)** not DCX. The 10× objective was used for **(K)**, the 20× objective was used for **(A, P–T)**, the 40× objective was used for **(B–E, L–O, U–Y)**, and the 63× objective was used for **(F–J)**.
AD-MSC: Adipose-derived mesenchymal stem cells; BDNF: Brain-derived neurotrophic factor; DAPI: 4, 6-Diamidino-2-phenylindole; DCX: Doublecortin; HuMi: Antihuman mitochondria; vWF: Von Willebrandt Faktor.

previously [59,60]. This fact also might lead to false absolute numbers of AD-MSC surviving in the brain over a long period of time, so in this study qualitative but no absolute quantitative characterization of AD-MSC was provided. Furthermore, AD-MSC localized predominantly in the arachnoid mater, which contains trophic factors [42,61] and might function as a stem-cell niche [42,62–63] supporting stem/precursor cell migration and distribution [64]. Therefore, it could be suggested that the arachnoid mater localization of AD-MSC supported or even enabled their long-term survival.

A progressive decrease or even a complete disappearance of MSC grafts is seen frequently in rat models [22,31–35], making long-term analyses difficult to validate. Regarding genetically engineered MSC, one of the underlying factors contributing to disappearing grafts might be a decrease in transgene expression. We showed previously that human specific marker give reliable and valid staining results by robust costaining with GFP, yet shortly after transplantation some AD-MSC stopped expressing GFP, but remained positive for human markers [29]. Gene silencing has been shown repeatedly in adult stem cells [65–67]. Consequently, additional human markers are essential to reliably track MSC. Our study used three different human specific markers to verify true AD-MSC survival and phenotyping. The fact that all AD-MSC stopped expressing GFP *in vivo* but not *in vitro* most likely reflects changes in the epigenetic state of the transgene, corresponding to their remarkable remodeling capacity that is indicated by their apparent microenvironmentally dependent transdifferentiation potential. Nevertheless, we were able to detect the AD-MSC 6 months after transplantation, but could not provide a reliable quantification of the cells at certain time points or the decrease in absolute numbers of AD-MSC over time, hence a correlation of the changing numbers of

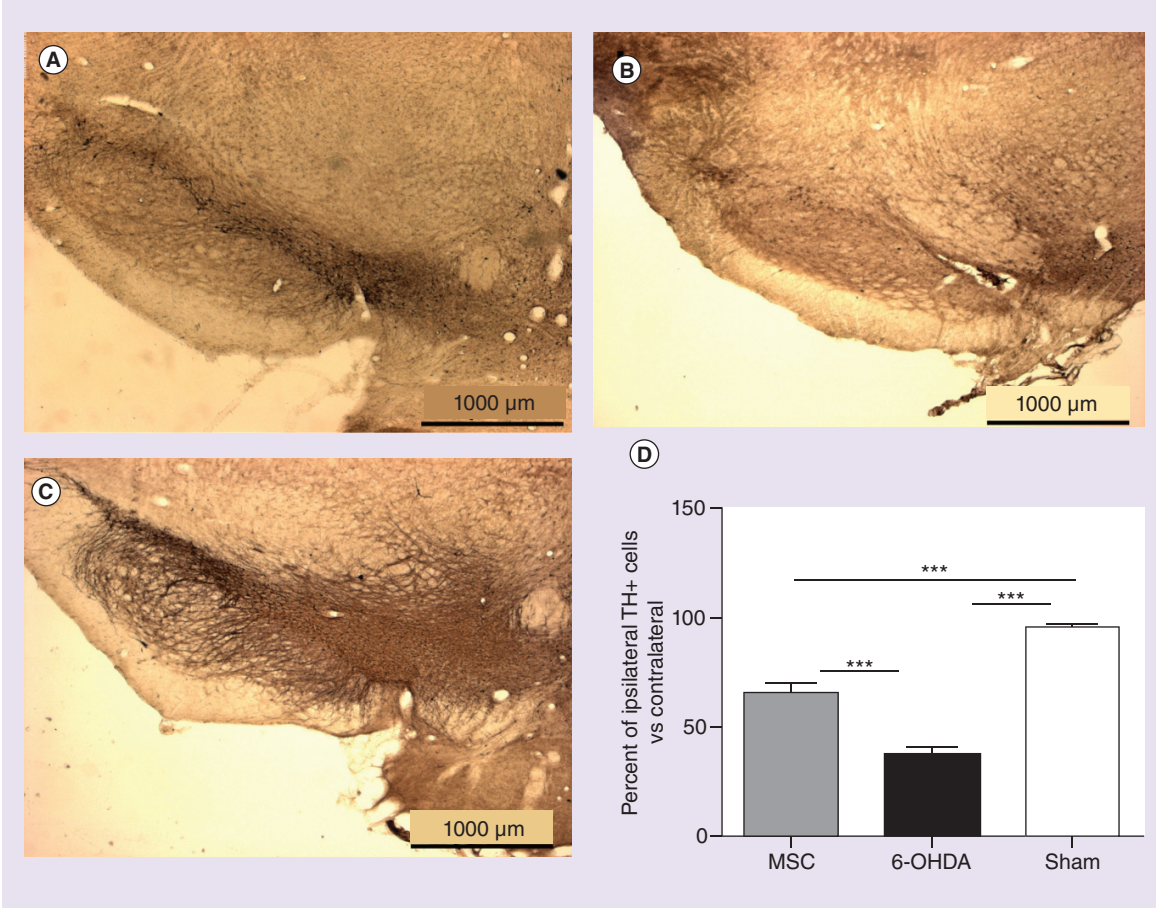

Figure 9. TH+ cells in the substantia nigra. TH-immunoreactive cells in the substantia nigra of **(A)** AD-MSC, **(B)** 6-OHDA and **(C)** sham transplanted animals. **(D)** Graphs of percentages of TH+ cells in the lesioned substantia nigra (ANOVA, $p < 0.000$), showing significantly decreased ipsilateral nigral TH+ neurons of 6-OHDA lesioned animals ($n = 7$), as compared with adipose-derived MSC ($n = 14$, $p = 0.000$) transplanted animals and as compared with sham lesioned animals ($n = 7$, $p = 0.000$), and significantly higher TH-levels in sham versus adipose-derived MSC ($p = 0.000$). The 2.5× objective was used for all.*** Indicating $p < 0.0005$.
6-OHDA: 6-Hydroxydopamine; MSC: Mesenchymal stem cells.

AD-MSC over time with the described histological and behavioral effects remain speculative.

In sum, our results showed that AD-MSC transplantation – which could be tracked over a long-term period of 6 months – leads to improvements on cognitive performance, increased TH levels, subventricular and hippocampal neurogenesis and increased the content of anti-inflammatory factors. This suggests a neuroprotective effect of AD-MSC in PD models, along with the potential of inducing endogenous repair programs in both neurogenic niches of the adult brain, potentially leading to improvements in nonmotor symptoms of PD, which affect patients early and hence represent a potential disease-modifying target.

Future perspective

The detection of adult MSC in 1970 [68] has brought a lot of new insights and new ways of application of adult stem cells. Not only their autologous potential and their ease of extraction and expansion have gained a lot of interest by colleagues in the field; primarily their profound effects on immunomodulation and their capacity to home toward injured structures without the risk of teratoma formation or other carcinogenic properties, have made these adult stem cells a very promising application for many types of diseases, including multiple sclerosis, chronic Graft Versus Host Disease and PD. The homing capacity of MSC also predisposes these cells as ideal vehicles for targeted vector delivery, for example, for delivering neurotrophic factors or other proteins of interest. Yet, how MSC are migrating in pathological and physiological states is still elusive and will be a very exciting topic in the next years [69], starting with the exploration of chemotactic pathways and interactions of MSC with the microenvironment.

Another aspects that will probably be examined in more detail in the near future are alternative routes of

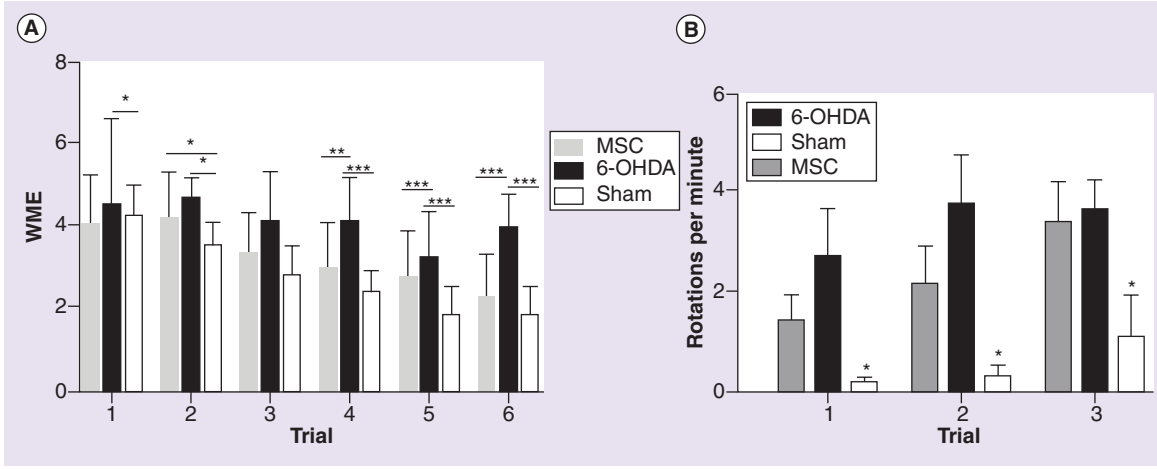

Figure 10. Radial-arm maze test and amphetamine-induced rotations. (A) Graphs showing a learning curve, with lower reference memory errors and WME with consecutive trials (p = 0.00 and p = 0.02) and significantly more WME in the 6-OHDA groups as compared with the adipose-derived MSC group (p = 0.001), and as compared with the sham control group (p = 0.000). **(B)** Graphs are indicating rotations per minute (rpm) averages over three test trials. Sham groups scored significantly lower than adipose-derived MSC (p = 0.02) and 6-OHDA (p = 0.007) groups. *** Indicating p < 0.0005; ** indicating p < 0.005; * indicating p < 0.05.
6-OHDA: 6-Hydroxydopamine; MSC: Mesenchymal stem cells; WME: Working memory errors.

MSC application. As shown by many studies, MSC are able to migrate, and hence might be able to pass the blood–brain barrier (BBB) when aided by other concomitantly infused compounds to open that barrier, for example, via receptor-mediated endocytosis/transcytosis [70]. Consequently, invasive procedures to apply these cells could be exchanged by more uncomplicated ways of application, once the mechanisms of MSC migration are better understood and can be guided more easily, for example, by the use of chemotaxis or by opening the BBB. Consequently, the amount of infused cells can be reduced if studies will use more tailored MSC that are designed for specific tissues and contexts. A combination of all these techniques would be ideal, for example, designing a chemotactic route for MSC, and – in the case of systemic administration – temporarily opening the BBB to allow a high infiltration into cerebral target structures.

Furthermore, during the next 5–10 years, there will be more information on the *in vivo* microenvironment, anatomic location and phenotype of MSC, elucidating their mechanisms of migration and their biological function, which will enable new approaches that intend to mobilize endogenous MSC in conditions of disease or neurodegeneration. In addition, understanding the biological functions of MSC could greatly help in tailoring cell therapies [71]. In line with this, the understanding of MSC biology will shift more away from progenitor functions and will be more defined to MSC paracrine and immune modulation effects. Comprehending the precise contexts of MSC regulation could greatly help to exploit MSC benefits,

Table 2. Radial Maze test results.

Type	Test day	AD-MSC	Sham control	6-OHDA lesion	Statistics
n		14	7	7	
	1	4(2)	2(0.5) p = 0.005†	6(3)	F(10, 44) = 2.13, p = 0.04, partial η^2 = 0.33
WME	2	3(2)	2(0.8) p = 0.05‡, p = 0.006†	4(1)	
	3	3(2)	2(0.8)	4(1)	
	4	2(1) p = 0.001§	1(0.7) p = 0.000†	4(1)	
	5	1(1) p = 0.000§	1(0.7) p = 0.000†	4(1)	
	6	0.6(1) p = 0.000§	0.8(0.6) p = 0.000†	5(1)	

†Indicating significant differences between sham control vs 6-OHDA.
‡Indicating significant differences between AD-MSC vs sham control.
§Indicating significant differences between AD-MSC vs 6-OHDA.
6-OHDA: 6-Hydroxydopamine; AD-MSC: Adipose-derived mesenchymal stem cells; WME: Working memory errors.

and these might be broadly applicable, including inflammatory, ischemic or degenerative diseases.

Hence, future studies will focus on improved therapeutic delivery methods of MSC, exploiting their biological functions and their chemotaxis to achieve safe ways of therapy. Furthermore, we anticipate that AD-MSC will gain more and more interest in the next 5–10 years, given their abundance, convenient isolation and cultivation, and their higher proliferative capacity, later senescence, and higher neurotrophin secretion than bone-marrow-derived MSC [23–25,72–74], making them the focus of most current MSC research.

Acknowledgements

Special thanks to M Hofstätter for her kind help with the construction of the GFP-vector.

Financial & competing interests disclosure

This study was funded by the ERFE grant of the Investitionsbank Berlin to B Steiner. The authors have no other relevant affiliations or financial involvement with any organization or entity with a financial interest in or financial conflict with the subject matter or materials discussed in the manuscript apart from those disclosed.

No writing assistance was utilized in the production of this manuscript.

Ethical conduct of research

The authors state that they have obtained appropriate institutional review board approval or have followed the principles outlined in the Declaration of Helsinki for all human or animal experimental investigations. In addition, for investigations involving human subjects, informed consent has been obtained from the participants involved.

Executive summary

Background

- Adipose-derived mesenchymal stem cells (AD-MSC) have been shown to be neuroprotective and might represent a new treatment approach in Parkinson's disease, yet, long-term results are missing.

Methods

- AD-MSC were transplanted into 6-hydroxydopamine lesioned rats and their effects were evaluated after 6 months.

Results

- AD-MSC survived up to 6 months in the lesioned substantia nigra and localized often in the arachnoid mater surrounding the brain and around blood vessel luminae.
- AD-MSC protected dopaminergic neurons, upregulated anti-inflammatory cytokines, and boosted neurogenesis and memory.
- The percent of dopaminergic neurons correlated positively with newly generated surviving neurons of the subventricular zone in all groups, indicating a relationship between the amount of dopaminergic neurons and subventricular neurogenesis.

Discussion

- AD-MSC could exert disease-modifying effects in Parkinson's disease, due to their modulatory effects on both adult neurogenic zones, while also protecting dopaminergic neurons.

References

Papers of special note have been highlighted as:
• of interest; •• of considerable interest

1 Schapira AH. Neurobiology and treatment of Parkinson's disease. *Trends Pharmacol. Sci.* 30(1), 41–47 (2009).

2 Braak H, Del Tredici K, Rub U, De Vos RA, Jansen Steur EN, Braak E. Staging of brain pathology related to sporadic Parkinson's disease. *Neurobiol. Aging* 24(2), 197–211 (2003).

3 Ubeda-Banon I, Saiz-Sanchez D, De La Rosa-Prieto C *et al.* alpha-Synucleinopathy in the human olfactory system in Parkinson's disease: involvement of calcium-binding protein- and substance P-positive cells. *Acta Neuropathol.* 119(6), 723–735 (2010).

4 Hoglinger GU, Rizk P, Muriel MP *et al.* Dopamine depletion impairs precursor cell proliferation in Parkinson disease. *Nat. Neurosci.* 7(7), 726–735 (2004).

•• **Essential study on neurogenesis, showing that precursor proliferation in the adult subependymal and subgranular zone depends on dopaminergic ennervation and is consequently reduced upon dopaminergic dennervation.**

5 Pearce RK, Hawkes CH, Daniel SE. The anterior olfactory nucleus in Parkinson's disease. *Mov. Disord.* 10(3), 283–287 (1995).

6 Aarsland D, Andersen K, Larsen JP, Lolk A, Kragh-Sorensen P. Prevalence and characteristics of dementia in Parkinson disease: an 8-year prospective study. *Arch. Neurol.* 60(3), 387–392 (2003).

7 Camicioli R, Moore MM, Kinney A, Corbridge E, Glassberg K, Kaye JA. Parkinson's disease is associated with hippocampal atrophy. *Mov. Disord.* 18(7), 784–790 (2003).

8 Doty RL. Olfactory dysfunction in Parkinson disease. *Nat. Rev. Neurol.* 8(6), 329–339 (2012).

9 Lesemann A, Reinel C, Huhnchen P *et al.* MPTP-induced hippocampal effects on serotonin, dopamine, neurotrophins, adult neurogenesis and depression-like behavior are partially influenced by fluoxetine in adult mice. *Brain Res.* 1457, 51–69 (2012).

10 Tansey MG, Goldberg MS. Neuroinflammation in Parkinson's disease: its role in neuronal death and implications for therapeutic intervention. *Neurobiol. Dis.* 37(3), 510–518 (2010).

11 Yasuhara T, Shingo T, Muraoka K *et al.* Neurorescue effects of VEGF on a rat model of Parkinson's disease. *Brain Res.* 1053(1–2), 10–18 (2005).

12 Zhou QH, Hui EK, Lu JZ, Boado RJ, Pardridge WM. Brain penetrating IgG-erythropoietin fusion protein is neuroprotective following intravenous treatment in Parkinson's disease in the mouse. *Brain Res.* 1382, 315–320 (2011).

13 Ma S, Xie N, Li W, Yuan B, Shi Y, Wang Y. Immunobiology of mesenchymal stem cells. *Cell Death Different.* 21(2), 216–225 (2013).

14 Boomsma RA, Geenen DL. Mesenchymal Stem Cells Secrete Multiple Cytokines That Promote Angiogenesis and Have Contrasting Effects on Chemotaxis and Apoptosis. *PLoS ONE* 7(4), e35685 (2012).

15 Kilroy GE, Foster SJ, Wu X *et al.* Cytokine profile of human adipose-derived stem cells: expression of angiogenic, hematopoietic, and pro-inflammatory factors. *J. Cell. Physiol.* 212(3), 702–709 (2007).

16 Abumaree M, Al Jumah M, Pace RA, Kalionis B. Immunosuppressive properties of mesenchymal stem cells. *Stem Cell Rev.* 8(2), 375–392 (2012).

17 Devine SM, Bartholomew AM, Mahmud N *et al.* Mesenchymal stem cells are capable of homing to the bone marrow of non-human primates following systemic infusion. *Exp. Hematol.* 29(2), 244–255 (2001).

18 Mogi M, Togari A, Kondo T *et al.* Glial cell line-derived neurotrophic factor in the substantia nigra from control and parkinsonian brains. *Neurosci. Lett.* 300(3), 179–181 (2001).

19 Mogi M, Togari A, Kondo T *et al.* Brain-derived growth factor and nerve growth factor concentrations are decreased in the substantia nigra in Parkinson's disease. *Neurosci. Lett.* 270(1), 45–48 (1999).

20 Cova L, Armentero MT, Zennaro E *et al.* Multiple neurogenic and neurorescue effects of human mesenchymal stem cell after transplantation in an experimental model of Parkinson's disease. *Brain Res.* 1311, 12–27 (2010).

21 Park HJ, Shin JY, Lee BR, Kim HO, Lee PH. Mesenchymal stem cells augment neurogenesis in the subventricular zone and enhance differentiation of neural precursor cells into dopaminergic neurons in the substantia nigra of a parkinsonian model. *Cell Transplant.* 21(8), 1629–1640 (2012).

22 Coquery N, Blesch A, Stroh A *et al.* Intrahippocampal transplantation of mesenchymal stromal cells promotes neuroplasticity. *Cytotherapy* 14(9), 1041–1053 (2012).

23 Izadpanah R, Trygg C, Patel B *et al.* Biologic properties of mesenchymal stem cells derived from bone marrow and adipose tissue. *J. Cell. Biochem.* 99(5), 1285–1297 (2006).

24 Vidal MA, Walker NJ, Napoli E, Borjesson DL. Evaluation of senescence in mesenchymal stem cells isolated from equine bone marrow, adipose tissue, and umbilical cord tissue. *Stem Cells Dev.* 21(2), 273–283 (2012).

25 Zhang HT, Liu ZL, Yao XQ, Yang ZJ, Xu RX. Neural differentiation ability of mesenchymal stromal cells from bone marrow and adipose tissue: a comparative study. *Cytotherapy* 14(10), 1203–1214 (2012).

26 Mccoy MK, Martinez TN, Ruhn KA *et al.* Autologous transplants of Adipose-Derived Adult Stromal (ADAS) cells afford dopaminergic neuroprotection in a model of Parkinson's disease. *Exp. Neurol.* 210(1), 14–29 (2008).

27 Berg J, Roch M, Altschuler J *et al.* Human adipose-Derived Mesenchymal Stem Cells Improve Motor Functions and are Neuroprotective in the 6-Hydroxydopamine-Rat Model for Parkinson's Disease when Cultured in Monolayer Cultures but Suppress Hippocampal Neurogenesis and Hippocampal Memory Function when Cultured in Spheroids. *Stem Cell Rev.* 11(1), 133–149 (2014).

•• **Goundwork study for our study, which showed neuroprotective and effects of adipose-derived mesenchymal stem cells in a Parkinson's disease rat model.**

28 Ahmed H, Salem A, Atta H, Ghazy M, Aglan H. Do adipose tissue-derived mesenchymal stem cells ameliorate Parkinson's disease in rat model? *Hum. Exp. Toxicol.* 33(12), 1217–1231 (2014).

29 Schwerk A, Altschüler J, Roch M *et al.* Human adipose-derived mesenchymal stromal cells increase endogenous neurogenesis in the rat subventricular zone acutely after 6-hydroxydopamine lesioning. *Cytotherapy* 17(2), 199–214 (2015).

30 Frangioni JV, Hajjar RJ. *In vivo* tracking of stem cells for clinical trials in cardiovascular disease. *Circulation* 110(21), 3378–3383 (2004).

31 Glavaski-Joksimovic A, Virag T, Chang QA *et al.* Reversal of dopaminergic degeneration in a parkinsonian rat following micrografting of human bone marrow-derived neural progenitors. *Cell Transpl.* 18(7), 801–814 (2009).

32 Park HJ, Lee PH, Bang OY, Lee G, Ahn YH. Mesenchymal stem cells therapy exerts neuroprotection in a progressive animal model of Parkinson's disease. *J. Neurochem.* 107(1), 141–151 (2008).

• **Important study, which showed neuroprotective effects and a dopaminergic transdifferentiation of mesenchymal stem cells in a Parkinson's disease rat model.**

33 Wang W, Itaka K, Ohba S *et al.* 3D spheroid culture system on micropatterned substrates for improved differentiation efficiency of multipotent mesenchymal stem cells. *Biomaterials* 30(14), 2705–2715 (2009).

34 Weiss ML, Medicetty S, Bledsoe AR *et al.* Human umbilical cord matrix stem cells: preliminary characterization and effect of transplantation in a rodent model of Parkinson's disease. *Stem Cells* 24(3), 781–792 (2006).

35 Yuan H, Sarre S, Ebinger G, Michotte Y. Histological, behavioural and neurochemical evaluation of medial forebrain bundle and striatal 6-OHDA lesions as rat models of Parkinson's disease. *J. Neurosci. Methods* 144(1), 35–45 (2005).

36 Blandini F, Cova L, Armentero MT *et al.* Transplantation of undifferentiated human mesenchymal stem cells protects against 6-hydroxydopamine neurotoxicity in the rat. *Cell Transplant.* 19(2), 203–217 (2010).

37 Danielyan L, Schafer R, Von Ameln-Mayerhofer A *et al.* Therapeutic efficacy of intranasally delivered mesenchymal stem cells in a rat model of Parkinson disease. *Rejuvenation Res.* 14(1), 3–16 (2011).

38 Tepper JM, Damlama M, Trent F. Postnatal changes in the distribution and morphology of rat substantia nigra dopaminergic neurons. *Neuroscience* 60(2), 469–477 (1994).

39 Paxinos G, Watson C. *The Rat Brain in Stereotaxic Coordinates (5th Edition).* Elsevier Academic Pres, Amsterdam, The Netherlands (2005).

40 Ungerstedt U, Arbuthnott GW. Quantitative recording of rotational behavior in rats after 6-hydroxy-dopamine lesions of the nigrostriatal dopamine system. *Brain Res.* 24(3), 485–493 (1970).

41 Balschun D, Manahan-Vaughan D, Wagner T, Behnisch T, Reymann KG, Wetzel W. A specific role for group I mGluRs in hippocampal LTP and hippocampus-dependent spatial learning. *Learn. Mem.* 6(2), 138–152 (1999).

42 Decimo I, Fumagalli G, Berton V, Krampera M, Bifari F. Meninges. from protective membrane to stem cell niche. *Am. J. Stem Cells* 1(2), 92–105 (2012).

43 Nakagomi T, Molnar Z, Taguchi A *et al.* Leptomeningeal-derived doublecortin-expressing cells in poststroke brain. *Stem Cells Dev.* 21(13), 2350–2354 (2012).

44 Popescu BO, Gherghiceanu M, Kostin S, Ceafalan L, Popescu LM. Telocytes in meninges and choroid plexus. *Neurosci. Lett.* 516(2), 265–269 (2012).

45 Mercier F, Hatton GI. Connexin 26 and basic fibroblast growth factor are expressed primarily in the subpial and subependymal layers in adult brain parenchyma. roles in stem cell proliferation and morphological plasticity? *J. Compar. Neurol.* 431(1), 88–104 (2001).

46 Stylianopoulou F, Herbert J, Soares MB, Efstratiadis A. Expression of the insulin-like growth factor II gene in the choroid plexus and the leptomeninges of the adult rat central nervous system. *Proc. Natl Acad. Sci. USA* 85(1), 141–145 (1988).

47 Steiner B, Kronenberg G, Jessberger S, Brandt MD, Reuter K, Kempermann G. Differential regulation of gliogenesis in the context of adult hippocampal neurogenesis in mice. *Glia* 46(1), 41–52 (2004).

•• **Key paper on neurogenesis, which assessed the amount of neuronal precursors in proliferating cells of the dentate gyrus.**

48 Campos FL, Carvalho MM, Cristovao AC *et al.* Rodent models of Parkinson's disease: beyond the motor symptomatology. *Front. Behav. Neurosci.* 7, 175 (2013).

49 Domellof ME, Elgh E, Forsgren L. The relation between cognition and motor dysfunction in drug-naive newly diagnosed patients with Parkinson's disease. *Mov. Disord.* 26(12), 2183–2189 (2011).

50 Janvin CC, Larsen JP, Aarsland D, Hugdahl K. Subtypes of mild cognitive impairment in Parkinson's disease: progression to dementia. *Mov. Disord.* 21(9), 1343–1349 (2006).

51 Johnston LC, Su X, Maguire-Zeiss K *et al.* Human interleukin-10 gene transfer is protective in a rat model of Parkinson's disease. *Mol. Ther.* 16(8), 1392–1399 (2008).

52 Lundblad M, Andersson M, Winkler C, Kirik D, Wierup N, Cenci MA. Pharmacological validation of behavioural measures of akinesia and dyskinesia in a rat model of Parkinson's disease. *Eur. J. Neurosci.* 15(1), 120–132 (2002).

53 Meredith GE, Kang UJ. Behavioral models of Parkinson's disease in rodents: a new look at an old problem. *Mov. Disord.* 21(10), 1595–1606 (2006).

54 Chang JW, Wachtel SR, Young D, Kang UJ. Biochemical and anatomical characterization of forepaw adjusting steps in rat models of Parkinson's disease: studies on medial forebrain bundle and striatal lesions. *Neuroscience* 88(2), 617–628 (1999).

55 Sakanaka M, Wen TC, Matsuda S *et al. In vivo* evidence that erythropoietin protects neurons from ischemic damage. *Proc. Natl Acad. Sci. USA* 95(8), 4635–4640 (1998).

56 Wang L, Zhang ZG, Zhang RL *et al.* Matrix metalloproteinase 2 (MMP2) and MMP9 secreted by erythropoietin-activated endothelial cells promote neural progenitor cell migration. *J. Neurosci.* 26(22), 5996–6003 (2006).

57 Kiyota T, Ingraham KL, Swan RJ, Jacobsen MT, Andrews SJ, Ikezu T. AAV serotype 2/1-mediated gene delivery of anti-inflammatory interleukin-10 enhances neurogenesis and cognitive function in APP+PS1 mice. *Gene Ther.* 19(7), 724–733 (2012).

58 Perez-Asensio FJ, Perpina U, Planas AM, Pozas E. Interleukin-10 regulates progenitor differentiation and modulates neurogenesis in adult brain. *J. Cell Sci.* 126(Pt 18), 4208–4219 (2013).

59 Acquistapace A, Bru T, Lesault PF *et al.* Human mesenchymal stem cells reprogram adult cardiomyocytes toward a progenitor-like state through partial cell fusion and mitochondria transfer. *Stem Cells* 29(5), 812–824 (2011).

60 Nygren JM, Jovinge S, Breitbach M *et al.* Bone marrow-derived hematopoietic cells generate cardiomyocytes at a low frequency through cell fusion, but not transdifferentiation. *Nat. Med.* 10(5), 494–501 (2004).

61 Paredes MF, Li G, Berger O, Baraban SC, Pleasure SJ. Stromal-derived factor-1 (CXCL12) regulates laminar position of Cajal-Retzius cells in normal and dysplastic brains. *J. Neurosci.* 26(37), 9404–9412 (2006).

62 Decimo I, Bifari F, Rodriguez FJ *et al.* Nestin- and doublecortin-positive cells reside in adult spinal cord meninges and participate in injury-induced parenchymal reaction. *Stem Cells* 29(12), 2062–2076 (2011).

• **Essential study on neurogenesis showing that precursor proliferation in the adult subependymal and subgranular zone depends on dopaminergic ennervation and is consequently reduced upon dopaminergic dennervation.**

63 Nakagomi T, Molnar Z, Nakano-Doi A *et al.* Ischemia-induced neural stem/progenitor cells in the pia mater following cortical infarction. *Stem Cells Dev.* 20(12), 2037–2051 (2011).

64 Decimo I, Bifari F, Krampera M, Fumagalli G. Neural stem cell niches in health and diseases. *Curr. Pharm. Des.* 18(13), 1755–1783 (2012).

65 Bestor TH. Gene silencing as a threat to the success of gene therapy. *J. Clin. Invest.* 105(4), 409–411 (2000).

66 Ellis J, Yao S. Retrovirus silencing and vector design: relevance to normal and cancer stem cells? *Curr. Gene Ther.* 5(4), 367–373 (2005).

67 Pannell D, Ellis J. Silencing of gene expression: implications for design of retrovirus vectors. *Rev. Med. Virol.* 11(4), 205–217 (2001).

68 Friedenstein AJ, Chailakhjan RK, Lalykina KS. The development of fibroblast colonies in monolayer cultures of guinea-pig bone marrow and spleen cells. *Cell Tissue Kinet.* 3(4), 393–403 (1970).

69 Karp JM, Leng Teo GS. Mesenchymal stem cell homing: the devil is in the details. *Cell Stem Cell* 4(3), 206–216 (2009).

70 Pardridge WM, Boado RJ. Reengineering biopharmaceuticals for targeted delivery across the blood-brain barrier. *Methods Enzymol.* 503, 269–292 (2012).

71 Nerem RM. Cell-based therapies: from basic biology to replacement, repair, and regeneration. *Biomaterials* 28(34), 5074–5077 (2007).

72 Ikegame Y, Yamashita K, Hayashi S *et al.* Comparison of mesenchymal stem cells from adipose tissue and bone marrow for ischemic stroke therapy. *Cytotherapy* 13(6), 675–685 (2011).

73 Mizuno H, Hyakusoku H. Mesengenic potential and future clinical perspective of human processed lipoaspirate cells. *J. Nippon Med. Sch.* 70(4), 300–306 (2003).

74 Niemeyer P, Kornacker M, Mehlhorn A *et al.* Comparison of immunological properties of bone marrow stromal cells and adipose tissue-derived stem cells before and after osteogenic differentiation *in vitro*. *Tissue Eng.* 13(1), 111–121 (2007).